JBC RESEARCH ARTICLE

# Prostaglandin F2α and angiotensin II type 1 receptors exhibit differential cognate G protein coupling regulation

Received for publication, May 3, 2022, and in revised form, July 19, 2022 Published, Papers in Press, July 21, 2022,
https://doi.org/10.1016/j.jbc.2022.102294

**Dana Sedki[1], Aaron Cho[1], Yubo Cao[2], Ljiljana Nikolajev[2], N. D. Prasad Atmuri[3], William D. Lubell[3], and Stéphane A. Laporte[1,2,*]**

*From the [1]Department of Medicine, Research Institute of the McGill University Health Center, and [2]Department of Pharmacology and Therapeutics, McGill University, Montréal, Canada; [3]Department of Chemistry, University of Montréal, Montréal, Canada*

Edited by Kirill Martemyanov

**Promiscuous G protein–coupled receptors (GPCRs) engage multiple Gα subtypes with different efficacies to propagate signals in cells. A mechanistic understanding of Gα selectivity by GPCRs is critical for therapeutic design, since signaling can be restrained by ligand–receptor complexes to preferentially engage specific G proteins. However, details of GPCR selectivity are unresolved. Here, we investigated cognate G protein selectivity using the prototypical promiscuous Gαq/11 and Gα12/13 coupling receptors, angiotensin II type I receptor (AT1R) and prostaglandin F2α receptor (FP), bioluminescence resonance energy transfer–based G protein and pathway-selective sensors, and G protein knockout cells. We determined that competition between G proteins for receptor binding occurred in a receptor- and G protein–specific manner for AT1R and FP but not for other receptors tested. In addition, we show that while Gα12/13 competes with Gαq/11 for AT1R coupling, the opposite occurs for FP, and Gαq-mediated signaling regulated G protein coupling only at AT1R. In cells, the functional modulation of biased ligands at FP and AT1R was contingent upon cognate Gα availability. The efficacy of AT1R-biased ligands, which poorly signal through Gαq/11, increased in the absence of Gα12/13. Finally, we show that a positive allosteric modulator of Gαq/11 signaling that also allosterically decreases FP–Gα12/13 coupling, lost its negative modulation in the absence of Gαq/11 coupling to FP. Together, our findings suggest that despite preferential binding of similar subsets of G proteins, GPCRs follow distinct selectivity rules, which may contribute to the regulation of ligand-mediated G protein bias of AT1R and FP.**

G protein–coupled receptors (GPCRs) are membrane proteins that control numerous physiological processes. Upon binding to extracellular stimuli, such as hormones and drugs, GPCRs relay signals by engaging intracellular signaling regulators, namely, heterotrimeric G proteins (αβγ subunits) and β-arrestins (1, 2). Ligand-mediated activation of GPCRs enables functional dissociation of the Gα subunit from the heterotrimeric G protein, triggering activation of downstream signaling effectors.

Based on the nature of their α subunits, G proteins are classified into four major families: Gαs, Gαi/o, Gαq/11, and Gα12/13. Different G proteins activate specific downstream effectors that ultimately produce diverse signaling events. While many receptors specifically couple to a single G protein family, others show promiscuity and engage multiple different G protein subtypes. Recent pharmacological advances have revealed that signaling through promiscuous GPCRs can be directed by ligands to selectively engage specific G proteins, a strategy that can be useful therapeutically (3, 4). Therefore, understanding the mechanisms dictating preferred G protein coupling by promiscuous GPCRs in cells is pivotal for designing ligands with honed functional selectivity.

Despite considerable efforts, our knowledge remains limited regarding the fundamentals of GPCR-G protein selectivity. Information regarding the selectivity of GPCRs for different G proteins has been gleaned using various sensors, sequence homology analyses, and structural comparisons of interacting domains of receptors and G proteins (5–8). For example, the G protein C-terminal α5 helix has been identified as a site dictating receptor selectivity (9, 10). The orientation adopted by the C terminus of Gα upon receptor coupling correlates with the strength of the GPCR-G protein interaction, supporting cognate G protein interactions (11). Other regions within the G protein core have been shown to contribute to receptor selectivity (12, 13). These findings provide valuable insights for understanding cognate *versus* noncognate G protein recognition by GPCRs. However, few details are known concerning the selectivity between cognate G protein binding at promiscuous GPCRs. The study of the dynamic competition among cognate G proteins for promiscuous GPCRs is especially challenging due in part to variations in receptor and G protein expression amongst different cell and tissue types (14–16). Moreover, overexpression of G proteins has been shown to affect ligand efficacy and the biased signaling profile of GPCRs, such as the angiotensin II (AngII) type 1 receptor (AT1R) (15, 17, 18). The rules governing the impact of one G protein on the coupling efficacy of another cognate G protein remain to be elucidated for different promiscuous GPCRs.

Here, we studied the two promiscuous Gαq/11 and Gα12/13 receptors: AT1R and the prostaglandin F2α (PGF2α)

* For correspondence: Stéphane A. Laporte, stephane.laporte@mcgill.ca.

receptor (FP). These GPCRs, both found in smooth muscle cells, regulate contraction through these different G protein families and have exhibited ligand functional selectivity (19–21). Using CRISPR–Cas9 cell lines depleted of Gαq/11 and Gα12/13 and the selective complementation of G proteins, we show that G proteins compete differentially at these promiscuous GPCRs by distinct mechanisms.

## Results

### *Gα13 impedes Gαq coupling and signaling through AT1R but not FP*

We first evaluated G protein coupling profiles for FP and AT1R in human embryonic kidney 293 (HEK293) cells using Gαq/11, Gα12/13, and Gαi bioluminescence resonance energy transfer (BRET)–based sensors that measure Gα and Gβγ subunit dissociation (21). For both receptors, we observed a more robust Gαq BRET signal compared with that of Gα11 (Fig. S1*A*). For AT1R, a similar efficacy in BRET response to Gα12 and Gα13 was observed, whereas the FP receptor showed a better Gα13 response (Fig. S1*B*). Only AT1R efficiently engaged Gαi2 and Gαi3 (Fig. S1*C*). Because G protein coupling to receptors can be modulated by β-arrestin's interaction with receptors, we also assessed the ability of both FP and AT1R to engage β-arrestin1 and β-arrestin2 using a BRET-based membrane translocation assay (22). As previously reported, only AT1R recruits β-arrestins (23) (Fig. S1*D*).

Because FP and AT1R are both Gαq/11- and Gα12/13-coupled receptors, we next investigated how each G protein subtype influences the coupling and activation of its alternate cognate G proteins. We focused on Gαq and Gα13, as representatives of each of their respective G protein families, because of their high efficiency in binding both GPCRs. We also assessed the effect of Gα13 expression on FP- and AT1R-dependent Gαq activation in Gα12/13-depleted cells (ΔGα12/13 cells) to mitigate any confounding effects of endogenous Gα12/13. Agonist dose–response curves with the Gαq BRET sensor were generated and maximal responses between conditions were compared. We reasoned that this would allow us to compare G protein coupling efficacy to fully engaged ligand–receptor complexes. FP coupling to Gαq was unaltered in these cells compared with parental cells, where FP was similarly expressed (Figs. 1*A* and S2*A*). Reintroducing Gα13 in ΔGα12/13 cells led to more FP signaling through this pathway as revealed by the recruitment at the plasma membrane of the Gα12/13-dependent BRET PDZRhoGEF sensor (Fig. S3, *A* and *B*) (8). However, reintroducing Gα13 did not show differences in FP coupling efficacy to Gαq compared with receptors expressed alone in ΔGα12/13 cells (Fig. 1*B*). Remarkably, however, Gαq coupling to AT1R was significantly increased in ΔGα12/13 cells, compared with parental cells, despite AT1R being expressed at similar levels in both cell types (Figs. 1, *C* and S2*B*). Moreover, reintroducing Gα13 in ΔGα12/13 cells impeded Gαq activation by AT1R (Fig. 1*D*), whereas overexpressing the noncognate Gαs protein had no effect on Gαq coupling to either FP or AT1R (Fig. 1, *B* and *D*). The effect of Gα13 on receptor coupling and signaling through Gαq was also investigated by measuring the recruitment of its effector p63RhoGEF at plasma membrane and ensuing BRET signal (21). Similar effects to those seen with the Gαq sensor were observed (Fig. S4). Gα13 had no effect on FP-mediated Gαq activity (Fig. S4, *A* and *B*), unlike AT1R, where Gα13 expression significantly attenuated signaling through this pathway (Fig. S4, *C* and *D*). Because AT1R also couples to Gα12 and Gαi (21), we tested the impact of those G protein subunits on Gαq signaling by AT1R. Like for Gα13, overexpression of Gα12 in ΔGα12/13 cells led to a reduction of Gαq signaling by AT1R (Fig. S5). Similar effects were observed with the overexpression of Gαi2, suggesting that Gαq signaling by AT1R is modulated by the presence of these cognate G proteins but not by the noncognate Gαs.

To exclude the possibility that Gα13-mediated signaling regulates Gαq activity by AT1R, we also tested whether Gαq coupling was altered when Rho or Rho-associated protein kinase (ROCK) were inhibited using C3 exoenzyme and Y27632, respectively. Neither treatment influenced FP nor AT1R coupling to Gαq (Fig. S6, *A* and *B*). Together, these results suggest that the effects (or lack thereof) observed herein reflect the distinctive intrinsic property of Gα13 to compete with Gαq at AT1R.

Because PKC and mitogen-activated protein kinase (MAPK) are known downstream effectors of Gαq-coupled receptors and are activated by FP and AT1R (20, 21), we investigated the effect of Gα13 binding at these receptors on the activation of these kinases. Consistent with what we observed, the expression of Gα13 negatively affected PKC activation by AT1R but not FP, as revealed by the use of a BRET sensor of this kinase (21) (Fig. S6, *C* and *D*). Moreover, Gαq-dependent MAPK downregulation by Gα13 was only observed for AT1R (Fig. S6, *E* and *F*). In the absence of Gα12/13, AT1R-mediated MAPK activation increased, while reintroducing Gα13 in these cells significantly inhibited this response (Fig. S6*F*). Taken together, these data imply that Gα13 impedes receptor–Gαq coupling and signaling at AT1R independently of its activity on RhoA and ROCK downstream effectors.

### *Gαq regulates receptor–Gα13 coupling and signaling for both FP and AT1R*

We next examined the extent to which Gαq affected Gα13 signaling by FP and AT1R using the Gα13 sensor in HEK293 cells bearing or lacking Gαq/11 (ΔGαq/11 cells). We confirmed that both receptor expression levels were not altered between the two cell types (Fig. S2). Interestingly, in the absence of Gαq/11, Gα13 coupling to both FP and AT1R was significantly potentiated compared with that of cells expressing Gαq/11 (Fig. 2, *A* and *C*), and this effect was reversed for both receptors following reintroduction of Gαq in ΔGαq/11 cells (Fig. 2, *B* and *D*). Gαq expression also restored FP- and AT1R-mediated signaling as measured by the p63RhoGEF and PKC sensors (Fig. S7, *A*–*C*). However,

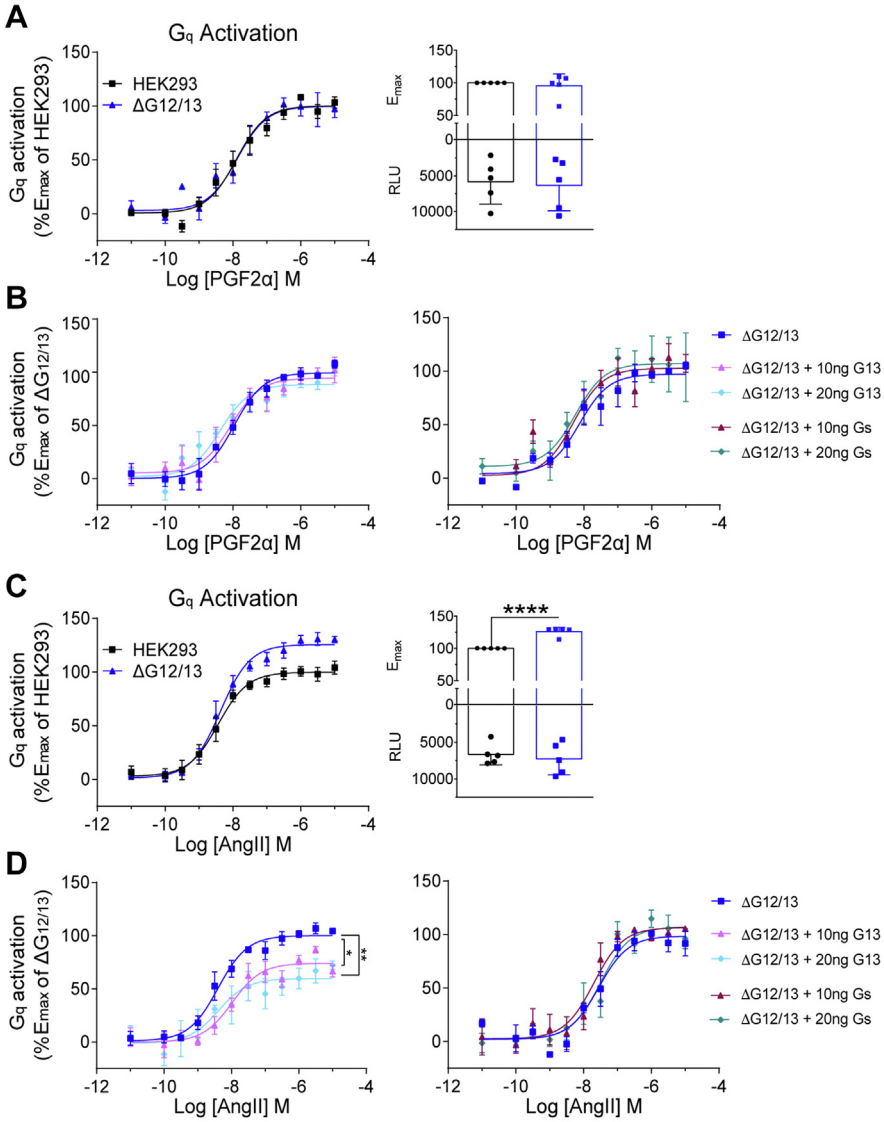


**Figure 1. Effect of Gα13 availability on Gαq activation by FP and AT1R.** *A–D*, Gαq activation following PGF2α stimulation of FP (*A* and *B*) or AngII stimulation of AT1R (*C* and *D*) assessed by the Gαq polycistronic sensor in HEK293 cells and ΔGα12/13 cells ± Gα13 (*B* and *D*, *left panels*) or Gαs (*B* and *D*, *right panels*) overexpression. BRET measurements are normalized to the maximal response in HEK293 cells (%$E_{max}$ of HEK293) (*A* and *C*) or in ΔGα12/13 cells without Gα overexpression (%$E_{max}$ of ΔG12/13) (*B* and *D*) in the same experiment. *A* and *C insets* show the expression levels of Gαq-RlucII (below *x*-axis) and the $E_{max}$ values of the dose–response curves (above *x*-axis). Data information: data are from at least three independent experiments and represent means ± SEM for the dose–response curves or ±SD for scatter plot bar graphs. In *A* and *C*, unpaired Student's *t* test was performed on the $E_{max}$ values obtained from the nonlinear regression curves of the average data. ****$p < 0.0001$. In *B* and *D*, two-way ANOVA followed by Dunnett's multiple comparisons tests were performed for the last time points. *$p < 0.05$ and **$p < 0.01$. AngII, angiotensin II; AT1R, angiotensin II type I receptor; BRET, bioluminescence resonance energy transfer; FP, prostaglandin F2α receptor; HEK293, human embryonic kidney 293 cell line; PGF2α, prostaglandin F2α; RLU, relative light unit.

expressing the noncognate Gαs subunit in ΔGαq/11 cells had no effect on FP- and AT1R-mediated Gα13 coupling (Fig. 2, *B* and *D*). Gαq competition and the lack of Gαs effects on FP and AT1R coupling to Gα13 were recapitulated when assessing the response of the downstream Gα13-mediated PDZRhoGEF sensor for these receptors (Fig. S8, *A–D*).

### *Gαq binding to FP impedes Gα13 coupling, whereas signaling downstream of Gαq inhibits Gα13 signaling through AT1R*

PKC has been involved in GPCR desensitization (*i.e.*, reduced G protein coupling) through receptor phosphorylation, but the extent to which it regulates receptor–G protein selectivity is unclear (24). AT1R and FP both contain PKC phosphorylation sites (25, 26). As expected, activating PKC with phorbol 12-myristate 13-acetate significantly reduced Gαq, Gα13, and Gαi2 activity at AT1R (Figs. 3*B* and S9). Surprisingly, however, it had no effect on FP coupling and signaling through Gαq and Gα13 (Figs. 3*A*, and S9, *A* and *B*). Consistent with these observations, inhibiting PKC with Gö6983 significantly increased AT1R coupling to its cognate G proteins, whereas FP coupling to Gαq and Gα13 remained unchanged (Figs. 3, *A* and *B*, and S9). We next used the Gαq inhibitor YM254890 (YM), which prevents GDP release from the G protein and the high-affinity interaction between the Gαq and the agonist-bound receptor (27, 28). Interestingly,

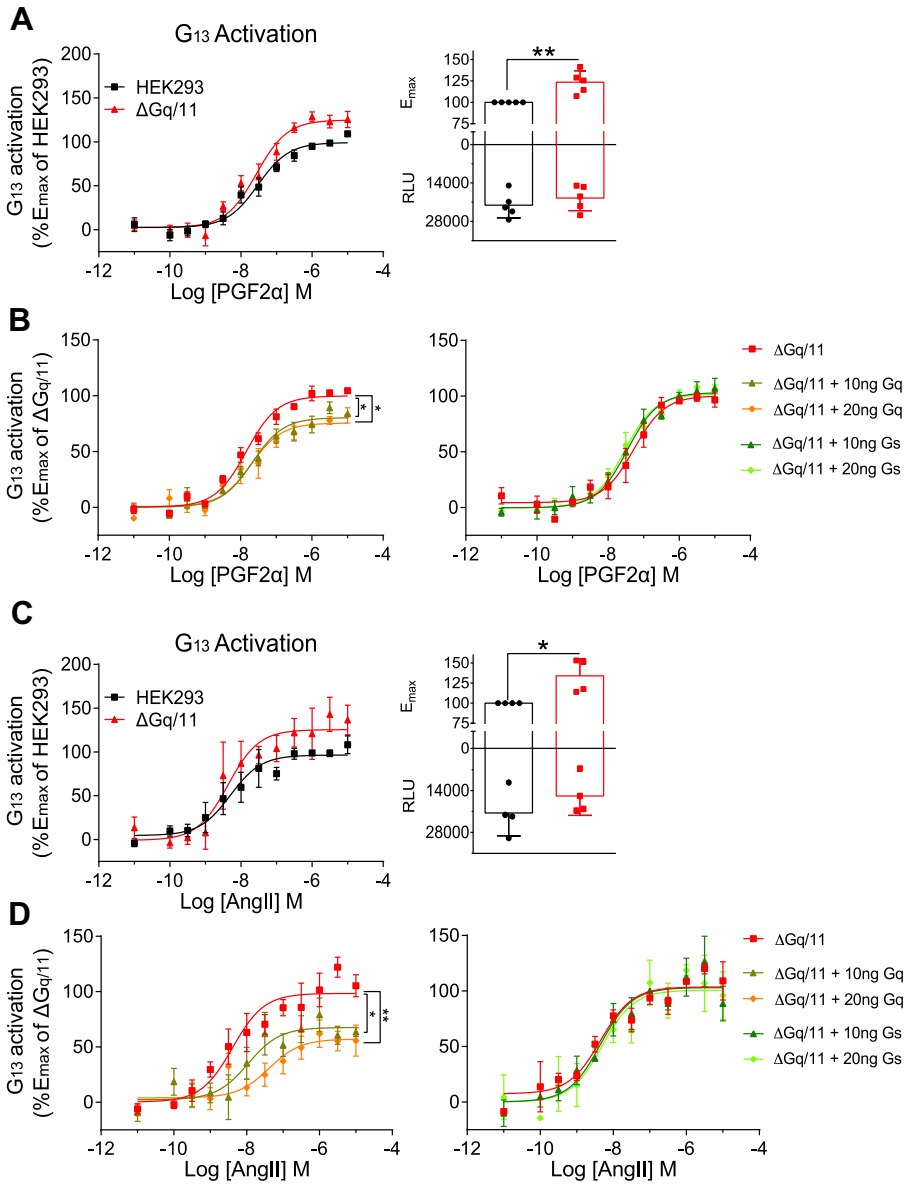


**Figure 2. Effect of Gαq availability on Gα13 activation by FP and AT1R.** *A–D*, Gα13 activation following PGF2α stimulation of FP (*A* and *B*) or AngII stimulation of AT1R (*C* and *D*) assessed by the Gα13 sensor in HEK293 cells and ΔGαq/11 cells ± Gαq (*B* and *D*, *left panels*) or Gαs (*B* and *D*, *right panels*) overexpression. BRET measurements are normalized to the maximal response in HEK293 cells (%$E_{max}$ of HEK293) (*A* and *C*) or in ΔGαq/11 cells without Gα overexpression (%$E_{max}$ of ΔGq/11) (*B* and *D*) in the same experiment. *A* and *C insets* show the expression levels of Gα13-RlucII (below *x*-axis) and the $E_{max}$ values of the dose–response curves (above *x*-axis). Data information: data are from at least three independent experiments and represent means ± SEM for the dose–response curves or ±SD for scatter plot bar graphs. In *A* and *C*, unpaired Student's *t* test was performed on the $E_{max}$ values obtained from the nonlinear regression curves of the average data. *$p < 0.05$, and **$p < 0.01$. In *B* and *D*, two-way ANOVA followed by Dunnett's multiple comparisons tests were performed for the last time points. *$p < 0.05$, and **$p < 0.01$. AngII, angiotensin II; AT1R, angiotensin II type I receptor; BRET, bioluminescence resonance energy transfer; FP, prostaglandin F2α receptor; HEK293, human embryonic kidney 293 cell line; PGF2α, prostaglandin F2α; RLU, relative light unit.

inhibiting receptor-dependent Gαq activation using YM significantly potentiated FP–Gα13 coupling efficacy and receptor signaling (Figs. 3*A* and S9*B*). Similarly, AT1R coupling to both Gα13 and Gαi2 was increased with YM treatment (Figs. 3*B* and S9, *B* and *C*). Together, these results suggest that while AT1R-G protein coupling is regulated by Gαq signaling, for FP, the extent of Gα13 coupling is independent of Gαq signaling but contingent on the ability of the latter G protein to compete with Gα13 for receptor binding.

To support these observations, we used the Q209L/D277N Gαq mutant (Q/D-Gαq), which lacks the ability to activate downstream effectors by mimicking the nucleotide-free Gα form (29). This Q/D-Gαq is nonetheless capable of binding receptors with high affinity, hence potentially competing with Gα13 for binding to FP. We also reasoned that because PKC and Gαq-mediated signaling should not be activated following AT1R coupling to Q/D-Gαq (Fig. S10, *A–C*), no inhibitory effect on receptor coupling to Gα13 should be observed. As predicted, expressing Q/D-Gαq in ΔGαq/11 cells only inhibited FP-mediated Gα13 binding and signaling (Fig. 3*C*), similar to what we observed when expressing a functional Gαq in these cells (Fig. S8*B*). Moreover, AT1R coupling and signaling

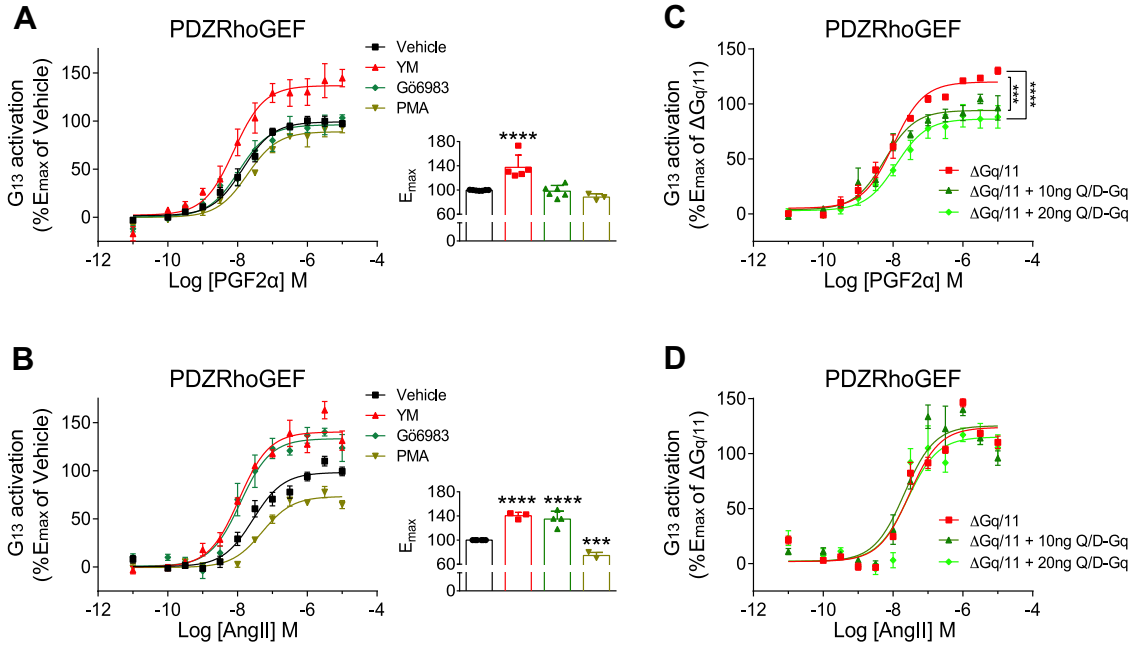


**Figure 3. Impact of Gαq downstream signaling on Gα13 activation by FP and AT1R.** *A–D*, Gα13-mediated PDZRhoGEF PM recruitment by FP (*A* and *C*) or AT1R (*B* and *D*) either in HEK293 cells treated with vehicle, 200 nM YM-254890 (YM), 1 μM Gö6983, or 1 μM PMA for 30 min (*A* and *B*) or in ΔGαq/11 cells ± inactive Gαq mutant (Q/D-Gαq) overexpression (*C* and *D*). Cells were stimulated with the indicated concentrations of PGF2α (*A* and *C*) or AngII (*B* and *D*). BRET measurements are normalized to the maximal response of vehicle-treated cells (%$E_{max}$ of vehicle) (*A* and *B*) or in ΔGαq/11 cells without Q/D-Gαq expression (%$E_{max}$ of ΔGq/11) in the same experiment. Data information: data are from at least three independent experiments and represent means ± SEM for the dose–response curves or ±SD for scatter plot bar graphs. In *A* and *B*, one-way ANOVA followed by Dunnett's multiple comparison test was performed on $E_{max}$ values obtained from the nonlinear regression curves of the averaged data. ***$p < 0.001$, and ****$p < 0.0001$. In *C* and *D*, two-way ANOVA followed by Dunnett's multiple comparisons tests were performed for the last time points. ***$p < 0.001$ and ****$p < 0.0001$. AngII, angiotensin II; AT1R, angiotensin II type I receptor; BRET, bioluminescence resonance energy transfer; FP, prostaglandin F2α receptor; HEK293, human embryonic kidney 293 cell line; PM, plasma membrane; PGF2α, prostaglandin F2α; PMA, phorbol 12-myristate 13-acetate.

through Gα13 was unaltered when Q/D-Gαq was overexpressed in these cells (Fig. 3*D*), which markedly contrasted with what we observed with the expression of a functional Gαq protein (Fig. S8*D*).

To further substantiate these observations, we next used an FP receptor mutant that is deficient in Gαq coupling (I147A/M247A; hereafter referred to as GαqNull-FP) (Fig. S11*A*). Despite GαqNull-FP being less well expressed than WT-FP in cells, it nonetheless showed a significant increase in Gα13 coupling and signaling, consistent with the lack of Gαq competition with Gα13 at the receptor (Figs. 4, *A* and *B*, and S11*B*). This finding is also in agreement with what we observed with WT-FP when Gαq/11 was absent from cells (ΔGαq/11 cells), or when Gαq was maintained in its inactive low receptor affinity state (*e.g.*, Gαq-GDP state following YM treatment) (Figs. 2*A* and 3*A*). Moreover, unlike WT-FP, the GαqNull–FP coupling to Gα13 was unchanged when the receptor was expressed in either HEK293 cells or ΔGαq/11 cells (Figs. 4, *C* and *D*, and 2*A*). Furthermore, GαqNull–FP-mediated Gα13 coupling and signaling were unaffected by reintroducing Gαq in ΔGαq/11 cells (Fig. 4, *E* and *F*). Altogether, these findings suggest that a direct Gαq–FP interaction is required for competing with Gα13 binding to this receptor.

### *Gα13 and Gαq competition are specific to FP and AT1R*

We further tested the extent to which Gαq and Gα13 competition and/or signaling regulated the coupling of other GPCRs to these G proteins. We used the bradykinin type 2 receptor (B2R) and the thromboxane A2 receptor alpha (TPα), which have been shown to couple to Gαq/11 and Gα12/13 (6, 8, 30). We first confirmed that B2R and TPα coupled to and activated Gαq/11 and Gα12/13 (Fig. S12, *A* and *B*). While loss of Gα13 competition with Gαq at AT1R in ΔGα12/13 cells increased receptor-mediated Gαq activation, it had no effects on either B2R or TPα signaling through Gαq, similar to FP (Fig. S12*C*). We also examined the effect of Gαq on Gα13-mediated signaling using either the Gαq knockout cells, or the Gαq and PKC inhibitors. Unlike for the FP and AT1R, B2R and TPα signaling through Gα13 was not potentiated neither in ΔGαq/11 cells nor with YM treatment (Fig. S12, *D* and *E*). Moreover, although PKC inhibition potentiated Gα13 signaling by AT1R, it had no effect on Gα13 signaling by neither B2R, nor TPα, similar to FP (Fig. S12*E*). Together, these results suggest that Gαq and Gα13 competition at GPCRs is specific for AT1R and FP.

### *Gα13 and Gαq competition influences the signaling profiles of FP and AT1R-biased ligands*

We have previously reported the identification of an allosteric modulator, PDC113.824 (PDC), which biases FP signaling by inhibiting Gα12/13 coupling while concomitantly increasing Gαq/11 signaling by the receptor (23). Considering our observation that Gαq competes with Gα13 coupling to FP, we reasoned that PDC exerts, in part, its bias function through such a mechanism. To investigate this

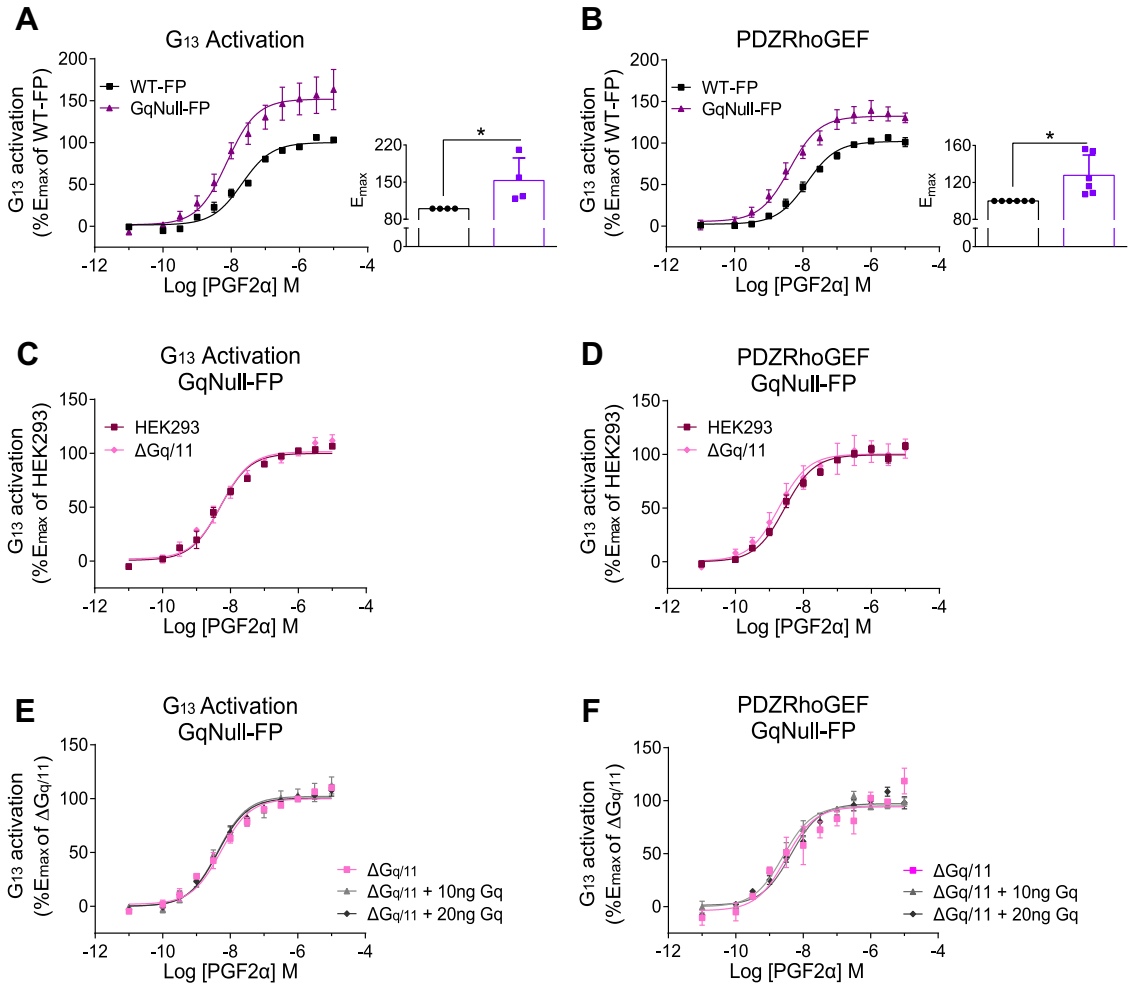


**Figure 4. Impact of Gαq availability on Gα13 signaling by the GαqNull mutant FP.** *A–F*, Gα13 activation assessed by the Gα13 sensor (*A*, *C*, and *E*), or by Gα13-mediated PDZRhoGEF PM translocation (*B*, *D*, and *F*) following PGF2α stimulation of WT-FP or GαqNull mutant FP (GαqNull-FP) in HEK293 cells (*A* and *B*) or of GαqNull-FP in HEK293 cells and ΔGαq/11 cells ± Gαq overexpression (*C–F*). BRET measurements are normalized to the maximal response of WT-FP (%$E_{max}$ of WT-FP) (*A* and *B*) or of GαqNull-FP in ΔGαq/11 cells without Gαq expression (%$E_{max}$ of ΔGq/11) in the same experiment. Data information: data are from at least three independent experiments and represent means ± SEM for the dose–response curves or ±SD for scatter plot bar graphs. In *A* and *B*, unpaired Student's *t* test was performed on $E_{max}$ values obtained from the nonlinear regression curve of the averaged data. *$p < 0.05$. BRET, bioluminescence resonance energy transfer; FP, prostaglandin F2α receptor; HEK293, human embryonic kidney 293 cell line; PGF2α, prostaglandin F2α; PM, plasma membrane.

possibility, we used a PDC analog, Az-PDC, which retained its positive allosteric modulation on the Gαq pathway as observed through the potentiation of FP-mediated MAPK signaling (Fig. S13, *A* and *B*), as well as its negative allosteric modulation on Gα13-mediated signaling by FP (Fig. 5*A*). As predicted, the negative allosteric modulation effect of Az-PDC on FP coupling to Gα13 was completely lost in cells expressing the WT receptor and lacking Gαq expression, as well as in cells expressing endogenous Gαq and over-expressing the GαqNull-FP (Fig. 5, *B–D*). We also tested the effect of two AngII analogs (TRV and SVdF) that produced preferential coupling of AT1R to Gα12/13 compared with Gαq/11 (21) (Fig. S13, *C* and *D*). Similar to AngII, TRV and SVdF coupling to Gαq was significantly increased in cells lacking Gα12/13 expression (Fig. 5*E*). These results further support the differential competition between Gαq and Gα13 at FP and AT1R and suggest a mechanism by which these ligands exert, in part, their bias function.

## Discussion

Using the two prototypical Gαq/11 and Gα12/13 receptors, AT1R and FP, we show that the availability of G proteins at these promiscuous GPCRs and their ensuing downstream signaling, in some cases, differentially regulate receptors coupling to their cognate G proteins (Fig. 6, *A–C*). Such regulation is dependent on the nature of the receptor and the G protein.

The directional and opposite regulation in Gαq and Gα12/13 competition at FP and AT1R supports a model where receptors bind their cognate G proteins with different affinities. Such directional regulation is also apparent when examining the effector responses downstream of these G proteins. These observations imply that G protein competition at these receptors neither results from an intrinsic property of the G protein sensors themselves nor is linked to the relative differences in endogenous Gαq/11 *versus* Gα12/13 levels, which may still exist. The lack of Gαq *versus* Gα13 competition in

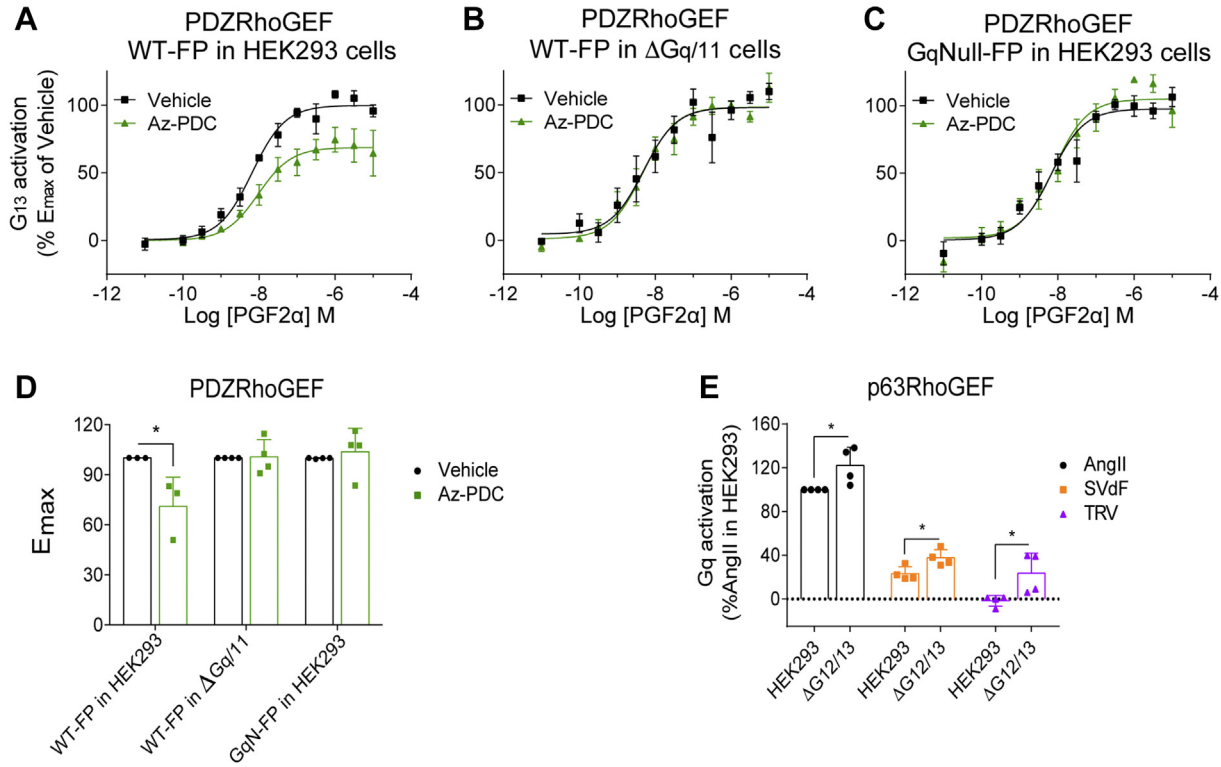


**Figure 5. Modulation of FP and AT1R-biased ligands with altered receptor G protein–binding availability.** *A–C*, Gα13-mediated PDZRhoGEF PM recruitment upon PGF2α stimulation of WT-FP (*A* and *B*) or GαqNull mutant FP (GαqNull-FP) (*C*) in parental HEK293 cells (*A* and *C*) or in ΔGαq/11 cells (*B*). Cells were pretreated with vehicle or 10 μM Az-PDC for 30 min prior to PGF2α stimulation with the indicated concentrations. BRET measurements are normalized to the maximal response in the vehicle-treated condition (%$E_{max}$ of vehicle). *D*, bar graph representation of $E_{max}$ values of the dose–response curves from *A–C*. *E*, Gαq-mediated p63RhoGEF PM recruitment upon AT1R stimulation in HEK293 cells or in ΔGα12/13 cells. Cells were stimulated with 10 μM of AngII, TRV, or SVdF. BRET measurements are normalized to the response of AngII (%$E_{max}$ of AngII). Data information: data are from at least three independent experiments and represent means ± SEM for the dose–response curves or ±SD for scatter plot bar graphs. In *D* and *E*, unpaired Student's *t* tests were performed. *$p < 0.05$. AngII, angiotensin II; AT1R, angiotensin II type I receptor; BRET, bioluminescence resonance energy transfer; FP, prostaglandin F2α receptor; HEK293, human embryonic kidney 293 cell line; PGF2α, prostaglandin F2α; PM, plasma membrane.

other GPCRs, such as the B2R and TPα receptors, also argues against these possibilities. It also suggests that affinities of these G protein subtype binding to B2R and TPα receptors may not greatly differ and/or that their binding requires distinct molecular determinants in these receptors than for AT1R and FP, where Gαq/11 and Gα12/13 may share more common binding modalities, hence showing competition. Whether this is also the case for other GPCRs that bind different cognate G proteins will need further investigation. Our findings also suggest that G protein competition does not necessarily involve the coupling of functional G proteins to receptors, reminiscent of the recently reported nonproductive G protein coupling to GPCRs (31). For AT1R, our data suggest a competition between G proteins at the receptor level and the regulation of cognate G protein interactions through signaling by PKC, consistent with receptor phosphorylation and desensitization (26, 32). However, our findings suggest that FP is neither subjected to such regulation nor β-arrestin participation in this process, unlike for AT1R, where β-arrestin could have had differential effects on G protein subtype competition at the receptor, something we did not investigate herein. Although our findings with AT1R and FP suggest differential competition between cognate G proteins at the receptor level, we cannot exclude the possibility that the recruitment of effectors to a receptor–G protein complex also interferes with the coupling of another cognate G protein. Also, the relocalization of receptors and the compartmentalization in cells of different signaling components, such as in lipid rafts or caveolae, could also alter receptor-coupling selectivity and contribute to the observed G protein competition (33). Finally, we cannot exclude in experiments using Gα-depleted cells or overexpressing Gα subunit that the nature and abundance of heterotrimer complexes may be altered, hence differentially affecting cognate G protein interactions with receptors.

Specific residues at the GPCR–G-protein interface not only play a role in determining selectivity (5, 9, 12) but also likely regulate the coupling strengths of different cognate G proteins to their receptor. Selectivity in G protein coupling also can emerge from the ability of GPCR–ligand complexes to differently sample distinct ensembles of conformations and to select for one G protein over another (11, 34). This may explain a mechanism by which biased ligands exert, in part, their differential effects on receptors' selective coupling to G proteins. Our findings also suggest that functional selectivity for FP and AT1R in addition involves G protein competition at these receptors. Such a model is supported by our observations that an allosteric modulator acting on FP, Az-PDC, which conceivably stabilizes conformations in

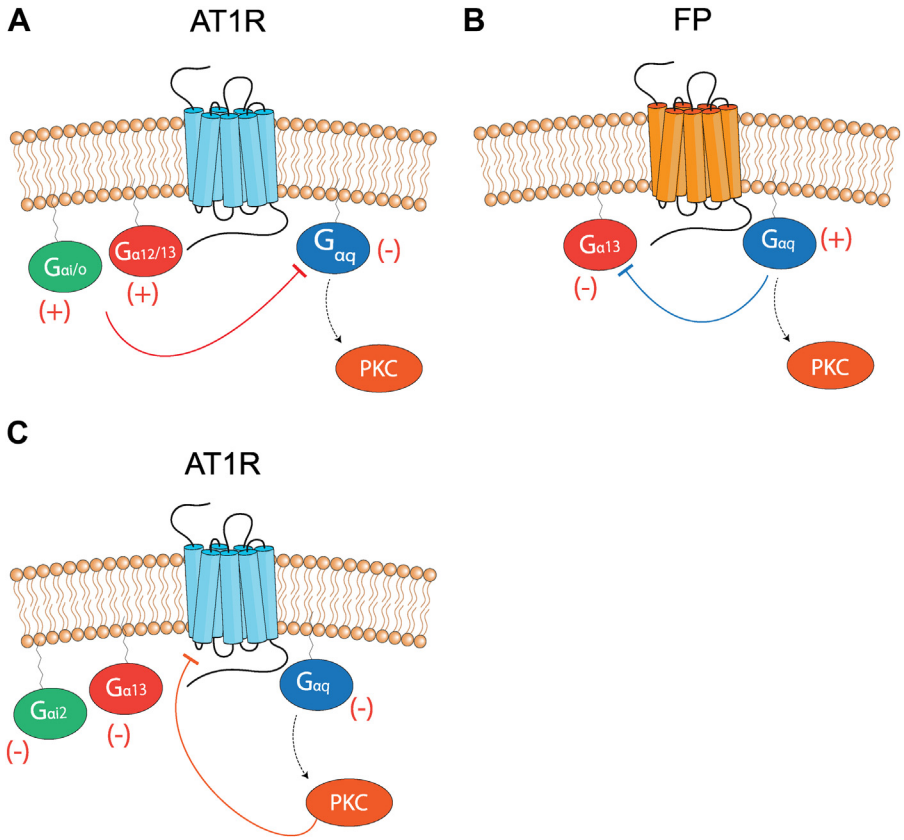


**Figure 6. Schematic representation of FP and AT1R selectivity regulation by G protein competitive coupling and/or signaling.** *A* and *B*, G proteins compete for receptor binding in a receptor-dependent fashion. For AT1R, Gαi2 and Gα12/13 binding restricts Gαq coupling and activation (*A*), whereas for FP, Gαq binding impedes Gα13 coupling and activation (*B*). *C*, Gαq, Gα13, and Gαi2 coupling to AT1R is regulated by PKC downstream of Gαq. AT1R, angiotensin II type I receptor; FP, prostaglandin F2α receptor.

the receptor favoring more efficient Gαq binding, reduces Gα13 coupling *via* a competition mechanism (20, 35). The absence of competition between Gαq and Gα13 coupling at B2R and TPα suggests that for these GPCRs, ligand–receptor complexes equally sample conformations that allow efficient binding of these two G protein families. Our findings also provide an explanation for how differential G protein availability in cells (*e.g.*, from different cell types) may alter not only the potency and efficacy of ligands but also bias profiles of ligands between systems (15, 17, 18). This is evidenced by our observation that AT1R ligands, which promote relatively better coupling to Gα12/13 over Gαq compared with AngII (21), showed increased Gαq coupling in the absence of Gα12/13 competition. These findings also provide a potential mechanism regarding how AT1R ligands negatively bias Gαq signaling, in addition to their ability to more efficiently engage β-arrestins. We propose that such a differential competitive mechanism can be further exploited to alter the G protein–biased profiles of allosteric and/or orthosteric drugs acting on AT1R and FP.

Gαq/11- and Gα12/13-mediated signaling by GPCRs, which contribute to myosin light chain phosphorylation through distinct and overlapping intermediate effectors such as Rho and ROCK, both contribute to coordinating smooth muscle contraction *in vivo*, although their relative involvement seems to differ in normal *versus* pathological settings (36). Our observation that Gαq and Gα13 differentially compete at AT1R and FP may have important implications in regulating smooth muscle and other cell contraction in normal physiology and pathophysiology, considering that G protein expression has been shown to vary in a cardiovascular disease model (15). Our results showing that biasing FP to increase its coupling to Gαq and ensuing competition with Gα13 binding is consistent with the observed inhibition of myometrial smooth muscle contraction *in vivo* (20). This questions, however, the relative roles of Gαq/11- and Gα12/13-dependent signaling in the regulation of uterine smooth muscle contraction during parturition. Moreover, we previously showed that agonist activation of either FP or AT1R in vascular smooth muscles increases the pressor response promoted by agonist activation of the other receptor, a phenomenon that was attributed to receptor heterodimerization but could also have involved differential regulation of Gαq/11 and Gα12/13 competition at FP and AT1R (19). Interestingly, Gα12/13-dependent signaling by vasocontractile GPCRs such as AT1R following vascular injury has been shown to prevent vascular smooth muscle dedifferentiation and proliferation, which is mediated by Gαq/11 signaling, hence playing an antagonistic cardiovascular protective role (37). It is therefore tempting to speculate that biased ligands such as TRV and SVdF that preserve Gα12/13 and β-arrestin coupling to AT1R (21), hence further limiting the activation of Gαq by the

receptor, could have better cardioprotective effects than ligands that interfere with all pathways or only the Gαq/11 pathway.

In summary, our findings not only reveal distinctive coupling profiles in FP and AT1R engaging the same families of cognate G proteins but also suggest different mechanisms of competitive regulation for G protein coupling to these receptors, where one cognate G protein can restrain the coupling of another one. Such findings may have important ramifications in drug development given the potential role of cognate G protein competition in regulating the functional bias of orthosteric ligands and allosteric modulators.

## Experimental procedures

### Reagents

PGFα, BK, and U46619 were from Cayman Chemical. TRV (Sar Arg Val Tyr Ile His Pro D-Ala) and SVdF (Sar Arg Val Tyr Val His Pro D-Phe) ligands were from GenScript. AngII, poly-L-ornithine, poly-L-lysine, and horseradish peroxidase–conjugated rabbit secondary antibodies were purchased from Sigma–Aldrich. Horseradish peroxidase–conjugated mouse secondary antibody was purchased from Bio-Rad. [$^3$H] PGF2α and chemiluminescence reagents were purchased from PerkinElmer Life Sciences. $^{125}$I-AngII (specific radioactivity ∼1000 Ci/mmol) was prepared with Iodo-GEN (Perbio-Science) as reported previously (21). Polyethylenimine was acquired from Polyscience, Inc. Coelenterazine was purchased from NanoLight Technology. YM-254890 was purchased from FUJIFILM Wako Chemicals USA, Corp. Gö6983 was acquired from Calbiochem. Y27632 is from Ascent. C3 exoenzyme is from Cytoskeleton. Anti-Gαq (10) and anti-Gα13 (A-20) antibodies were from Santa Cruz Biotechnology. Rabbit polyclonal anti–p-ERK and anti–total-ERK antibodies were from Cell Signaling. Az-PDC was synthesized at University of Montreal (38). Trypsin, PBS, Dulbecco's modified Eagle's medium, fetal bovine serum, gentamycin, and other cell culture reagents were acquired from Gibco, Life Technologies. Phusion DNA polymerase was from Thermo Scientific. Restriction enzymes, T4 DNA ligase, and Gibson assembly mix were obtained from New England Biolabs. Oligonucleotides were synthesized at Integrated DNA Technologies. All other reagents were obtained from Thermo Fisher Scientific and were of analytical grade.

### Plasmids and constructs

The polycistronic Gαq sensor, and the Gα12, Gα13, Gαi2, and Gαi3 BRET sensors were described elsewhere (21, 39, 40). The polycistronic Gα11 sensor was provided by Dr Michel Bouvier (University of Montreal). Briefly, GNA11 internally tagged with RlucII at position 127 was generated by overlap PCR, similar to the GNAo constructs. Gα11-RlucII was then cloned into the Gαq polycistronic BRET vector, replacing the Gαq sequence with that of Gα11. BRET sensors for β-arrestin1 and β-arrestin2 recruitment and PKC activation were described in (21, 22). PDZRhoGEF and p63RhoGEF sensors were described previously (8). The complementary DNA clone for nonfunctional human Gαq mutant (Q209L/D277N) was previously described (20). Mutations affecting FP coupling to Gαq such as I147A and M247A were identified from a whole receptor alanine mutagenesis screen (article in preparation). The GαqNull (I147A/M247A) mutant FP receptor (GαqNull-FP) was engineered by the two-part PCR mutagenesis strategy described previously (41, 42). Briefly, site-directed mutagenesis primers with 18 bp of Gibson homology for Gibson assembly recombination were generated and ordered from Integrated DNA Technologies. I147A mutation was first introduced, and the I147A FP mutant vector was then used as the template to generate the double mutant I147A/M247A in FP. Mutations were introduced through a step-down PCR; two separate PCRs were performed to split the vector in half. The two half PCR samples were combined, digested with DpnI, and purified. Samples of the two half vectors were then Gibson ligated. The reannealed vector was then transformed into bacteria, and one of the grown colonies was picked and amplified. Incorporation of mutations was verified by sequencing at Genome Québec, CES.

### Cell culture and transfections

HEK293 cells depleted in Gαq/11 (ΔGαq/11) and Gα12/13 (ΔGα12/13) were obtained from Dr Asuka Inou (Tohoku University) and previously described in (43). Cells were cultured in Dulbecco's modified Eagle's medium supplemented with 10% fetal bovine serum and 20 μg/ml gentamycin at 37 °C in 5% $CO_2$ and 90% humidity. Transient transfections were performed using the polyethylenimine method at a 3:1 ratio (w/w) with plasmid DNA on cells in suspension. For BRET experiments, cells were seeded onto polyornithine-coated white 96-well plates at a density of 20 × $10^3$ cells per well. Each 12 wells were transiently transfected with 150 ng receptor, along with one of the BRET sensors: 250 ng Gαq or Gα11 polycistronic sensors, or 15 ng Gα12-RlucII or Gα13-RlucII with 60 ng GFP10-Gγ1 and Gβ1 sensors, or 60 ng Gαi2-RlucII or Gαi3-RlucII with 60 ng GFP10-Gγ2 and Gβ2 sensors, or 15 ng of β-arrestin-1-RlucII or β-arrestin-2-RlucII with 60 ng of rGFP-CAAX sensors, or 60 ng PKC sensor, or 15 ng PDZRhoGEF-RlucII with 10 ng Gα13 and 60 ng of rGFP-CAAX sensor or 15 ng p63RhoGEF-RlucII with 10 ng Gαq and 60 ng of rGFP-CAAX sensor. For BRET experiments where Gα subunit is overexpressed, Gα13, Gαq, or Gαs were transfected either at 10 ng or 20 ng per 12 wells. For binding experiments, cells were seeded onto poly-L-lysine–coated 24-well plates at a density of 80 × $10^3$ cells per well and were transiently transfected with 600 ng/well of the appropriate receptor. For immunoblotting experiments, cells were seeded at a density of 160 × $10^3$ cells per well in 12 well plates and were transiently transfected with 1 μg FP or AT1Rs. In all experiments, the medium was replaced 18 h post-transfection, and the experiment was carried on 48 h post-transfection.

### Radioligand-binding experiments

Receptor abundance was assessed by ligand-binding assays using [$^3$H]-PGF2α or [$^{125}$I]-AngII in saturation experiments.

[$^{125}$I]-AngII was prepared using the Iodogen method, as previously described (44). For binding experiments, HEK293T, ΔGαq/11, and ΔGα12/13 cells transiently expressing the appropriate receptor were washed once with ice-cold PBS and incubated with or without 1 μM cold AngII or PGF2α and fixed concentrations of [$^{125}$I]-AngII (100,000 cpm at 1000 Ci/mmol) or [$^{3}$H]-PGF2α (150–240 Ci/mmol), respectively, in a total volume of 0.5 ml of binding buffer (50 mM Tris [pH 7.4], 5 mM $MgCl_2$, 100 mM NaCl, and 0.2% [w/v] bovine serum albumin [BSA]). Cells were incubated at room temperature for 1 h for [$^{125}$I]-AngII or at 4 °C overnight for [$^{3}$H]-PGF2α binding. Binding was stopped by washing cells three times with ice-cold PBS, and cells were lysed with NP-40 (for [$^{3}$H]) or 0.2 M NAOH (for [$^{125}$I]) for 10 min at room temperature. Incorporated radioactivity was then measured by a β-counter [$^{3}$H] or a γ-counter [$^{125}$I]. Receptor relative expression levels in the different cell lines were measured by subtracting the nonspecific binding (determined by the addition of cold ligands) from the total binding.

### BRET assays

Cells transfected with receptor and BRET sensors were washed once and incubated with Tyrode's buffer (140 mM NaCl, 2.7 mM KCl, 1 mM $CaCl_2$, 12 mM $NaHCO_3$, 5.6 mM D-glucose, 0.5 mM $MgCl_2$, 0.37 mM $NaH_2PO_4$, 25 mM Hepes, pH 7.4) for 30 min at 37 °C with 5% $CO_2$. For concentration–response and time-course experiments, cells were stimulated with various concentrations of PGF2α or AngII in Tyrode for 2 to 6 min or with a single concentration of the ligand for various durations ranging between 5 and 30 min. For the polycistronic Gαq and Gα11 sensors, and the Gαi2 and Gαi3, p63RhoGEF, PDZRhoGEF, and PKC sensors, stimulation was carried out at 2 min. For the Gα13 and Gα12 sensors, stimulation was performed for 6 and 10 min, respectively. For all BRET experiments, coelenterazine 400a was added at a final concentration of 5 μM 3 to 5 min prior, and BRET measurements were obtained using the Synergy2 (BioTek) plate reader with filter sets of 410/80 nm (donor) and 515/30 nm (acceptor). BRET ratio was calculated as the ratio of the intensity of acceptor light emission over the intensity of donor light emission.

### Western blotting

Two days post-transfection, cells were washed once with PBS, serum starved in Hepes containing media for 30 min at 37 °C, and stimulated with 1 μM of PGF2α or AngII. Stimulation was stopped by washing cells once with ice-cold PBS and lysing cells with Laemmli buffer (250 mM Tris–HCl [pH 6.8], 2% [w/v] SDS, 10% [v/v] glycerol, 0.01% [w/v] bromophenol blue, and supplemented with 5% [v/v] β-mercaptoethanol). For G protein overexpression experiments, cells were washed once with PBS and directly lysed with Laemmli buffer. Protein samples were then resolved by SDS-polyacrylamide gel electrophoresis. Membranes were incubated with primary rabbit polyclonal anti–phospho-44/42 ERK1/2, or anti-total ERK1/2 antibodies diluted in 1:1000 ratio in 1% BSA, or with mouse monoclonal anti-Gαq (10), or anti-Gα13 (A-20) antibodies diluted in 1:500 ratio in 1% BSA. Antibody incubation was done overnight at 4 °C on a nutating mixer. Secondary anti-rabbit or anti-mouse antibodies conjugated to horseradish peroxidase were then used to detect bands by chemiluminescence (1:10,000 dilution). Chemiluminescence signals were detected using Chemidoc Imaging System (Bio-Rad), and protein bands were quantified by densitometry analysis using Image Lab 6.0 (Bio-Rad). ERK phosphorylation was expressed as the relative ratio between the intensity of phospho-ERK1/2 to ERK1/2.

### Data analysis

All data were analyzed using Image Lab 6.0 (Bio-Rad) and Prism 6.0 (GraphPad Software, Inc). Statistical analyses were performed using Student's *t* tests, one- or two-way ANOVAs, and Dunnett's or Bonferroni's multiple comparisons test when appropriate. Statistical significance was considered when $p < 0.05$.

## Data availability

All data and analyses are included in the main text of the article and the supporting information.

*Supporting information*—This article contains supporting information.

*Acknowledgments*—We are grateful for the helpful discussions with all past and present members of the Laporte laboratory. We thank Drs Michel Bouvier and Christian Le Gouill from the University of Montreal for providing the p63RhoGEF-RlucII, the PDZRhoGEF-RlucII, and the Gα11 polycistronic constructs. We also thank Dr Asuka Inoue from Tohoku University for providing the ΔGαq/11 and ΔGα12/13 cells. This work was supported by grants from the Canadian Institutes of Health Research (grant nos.: PJT-162368 and PJT-173504).

*Author contributions*—D. S. and S. A. L. conceptualization; A. C. and L. N. validation; D. S. formal analysis; D. S. investigation; N. D. P. A and S. A. L. resources; D. S. and S. A. L. writing–original draft; A. C., Y. C., and W. D. L. writing–review & editing; Y. C. visualization; W. D. L. and S. A. L. supervision; S. A. L. funding acquisition.

*Funding and additional information*—D. S. was supported by the Maysie MacSporran graduate studentship from McGill University, and Y. C. was supported by a doctoral training scholarship of Fonds de recherche santé Québec.

*Conflict of interest*—Some of the BRET biosensors used in the present study are licensed to Domain Therapeutics for commercial use. The biosensors are freely available under material transfer agreement for academic research and can be requested from S. A. L. All other authors declare that they have no conflicts of interest with the contents of this article.

*Abbreviations*—The abbreviations used are: AngII, angiotensin II; AT1R, angiotensin II type I receptor; B2R, bradykinin type 2 receptor; BRET, bioluminescence resonance energy transfer; BSA,

bovine serum albumin; FP, prostaglandin F2α receptor; GPCR, G protein–coupled receptor; HEK293, human embryonic kidney 293 cell line; MAPK, mitogen-activated protein kinase; PDC, PDC113.824; PGF2α, prostaglandin F2α; Q/D-Gαq, Q209L/D277N Gαq mutant; ROCK, Rho-associated protein kinase; TPα, thromboxane A2 receptor alpha; YM, YM254890.

## References


1. Wettschureck, N., and Offermanns, S. (2005) Mammalian G proteins and their cell type specific functions. *Physiol. Rev.* **85**, 1159–1204
2. Shenoy, S. K., and Lefkowitz, R. J. (2011) beta-Arrestin-mediated receptor trafficking and signal transduction. *Trends Pharmacol. Sci.* **32**, 521–533
3. Slosky, L. M., Caron, M. G., and Barak, L. S. (2021) Biased allosteric modulators: new frontiers in GPCR drug discovery. *Trends Pharmacol. Sci.* **42**, 283–299
4. Khoury, E., Clement, S., and Laporte, S. A. (2014) Allosteric and biased g protein-coupled receptor signaling regulation: potentials for new therapeutics. *Front. Endocrinol. (Lausanne)* **5**, 68
5. Flock, T., Hauser, A. S., Lund, N., Gloriam, D. E., Balaji, S., and Babu, M. M. (2017) Selectivity determinants of GPCR-G-protein binding. *Nature* **545**, 317–322
6. Inoue, A., Raimondi, F., Kadji, F. M. N., Singh, G., Kishi, T., Uwamizu, A., *et al.* (2019) Illuminating G-protein-coupling selectivity of GPCRs. *Cell* **177**, 1933–1947.e1925
7. Masuho, I., Ostrovskaya, O., Kramer, G. M., Jones, C. D., Xie, K., and Martemyanov, K. A. (2015) Distinct profiles of functional discrimination among G proteins determine the actions of G protein-coupled receptors. *Sci. Signal.* **8**, ra123
8. Avet, C., Mancini, A., Breton, B., Le Gouill, C., Hauser, A. S., Normand, C., *et al.* (2022) Effector membrane translocation biosensors reveal G protein and betaarrestin coupling profiles of 100 therapeutically relevant GPCRs. *Elife* **11**
9. Semack, A., Sandhu, M., Malik, R. U., Vaidehi, N., and Sivaramakrishnan, S. (2016) Structural elements in the Galphas and Galphaq C termini that mediate selective G protein-coupled receptor (GPCR) signaling. *J. Biol. Chem.* **291**, 17929–17940
10. Conklin, B. R., Farfel, Z., Lustig, K. D., Julius, D., and Bourne, H. R. (1993) Substitution of three amino acids switches receptor specificity of Gq alpha to that of Gi alpha. *Nature* **363**, 274–276
11. Sandhu, M., Touma, A. M., Dysthe, M., Sadler, F., Sivaramakrishnan, S., and Vaidehi, N. (2019) Conformational plasticity of the intracellular cavity of GPCR-G-protein complexes leads to G-protein promiscuity and selectivity. *Proc. Natl. Acad. Sci. U. S. A.* **116**, 11956–11965
12. Okashah, N., Wan, Q., Ghosh, S., Sandhu, M., Inoue, A., Vaidehi, N., *et al.* (2019) Variable G protein determinants of GPCR coupling selectivity. *Proc. Natl. Acad. Sci. U. S. A.* **116**, 12054–12059
13. Alegre, K. O., Paknejad, N., Su, M., Lou, J. S., Huang, J., Jordan, K. D., *et al.* (2021) Structural basis and mechanism of activation of two different families of G proteins by the same GPCR. *Nat. Struct. Mol. Biol.* **28**, 936–944
14. Sriram, K., Moyung, K., Corriden, R., Carter, H., and Insel, P. A. (2019) GPCRs show widespread differential mRNA expression and frequent mutation and copy number variation in solid tumors. *PLoS Biol.* **17**, e3000434
15. Onfroy, L., Galandrin, S., Pontier, S. M., Seguelas, M. H., N'Guyen, D., Senard, J. M., *et al.* (2017) G protein stoichiometry dictates biased agonism through distinct receptor-G protein partitioning. *Sci. Rep.* **7**, 7885
16. Sungkaworn, T., Jobin, M. L., Burnecki, K., Weron, A., Lohse, M. J., and Calebiro, D. (2017) Single-molecule imaging reveals receptor-G protein interactions at cell surface hot spots. *Nature* **550**, 543–547
17. Kenakin, T. (1997) Differences between natural and recombinant G protein-coupled receptor systems with varying receptor/G protein stoichiometry. *Trends Pharmacol. Sci.* **18**, 456–464
18. Kenakin, T. (2002) Efficacy at G-protein-coupled receptors. *Nat. Rev. Drug Discov.* **1**, 103–110
19. Goupil, E., Fillion, D., Clement, S., Luo, X., Devost, D., Sleno, R., *et al.* (2015) Angiotensin II type I and prostaglandin F2alpha receptors cooperatively modulate signaling in vascular smooth muscle cells. *J. Biol. Chem.* **290**, 3137–3148
20. Goupil, E., Tassy, D., Bourguet, C., Quiniou, C., Wisehart, V., Petrin, D., *et al.* (2010) A novel biased allosteric compound inhibitor of parturition selectively impedes the prostaglandin F2alpha-mediated Rho/ROCK signaling pathway. *J. Biol. Chem.* **285**, 25624–25636
21. Namkung, Y., LeGouill, C., Kumar, S., Cao, Y., Teixeira, L. B., Lukasheva, V., *et al.* (2018) Functional selectivity profiling of the angiotensin II type 1 receptor using pathway-wide BRET signaling sensors. *Sci. Signal.* **11**, eaat1631
22. Namkung, Y., Le Gouill, C., Lukashova, V., Kobayashi, H., Hogue, M., Khoury, E., *et al.* (2016) Monitoring G protein-coupled receptor and beta-arrestin trafficking in live cells using enhanced bystander BRET. *Nat. Commun.* **7**, 12178
23. Goupil, E., Wisehart, V., Khoury, E., Zimmerman, B., Jaffal, S., Hebert, T. E., *et al.* (2012) Biasing the prostaglandin F2alpha receptor responses toward EGFR-dependent transactivation of MAPK. *Mol. Endocrinol.* **26**, 1189–1202
24. Lefkowitz, R. J. (1998) G protein-coupled receptors. III. New roles for receptor kinases and beta-arrestins in receptor signaling and desensitization. *J. Biol. Chem.* **273**, 18677–18680
25. Srinivasan, D., Fujino, H., and Regan, J. W. (2002) Differential internalization of the prostaglandin f(2alpha) receptor isoforms: role of protein kinase C and clathrin. *J. Pharmacol. Exp. Ther.* **302**, 219–224
26. Qian, H., Pipolo, L., and Thomas, W. G. (1999) Identification of protein kinase C phosphorylation sites in the angiotensin II (AT1A) receptor. *Biochem. J.* **343 Pt 3**, 637–644
27. Schrage, R., Schmitz, A. L., Gaffal, E., Annala, S., Kehraus, S., Wenzel, D., *et al.* (2015) The experimental power of FR900359 to study Gq-regulated biological processes. *Nat. Commun.* **6**, 10156
28. Nishimura, A., Kitano, K., Takasaki, J., Taniguchi, M., Mizuno, N., Tago, K., *et al.* (2010) Structural basis for the specific inhibition of heterotrimeric Gq protein by a small molecule. *Proc. Natl. Acad. Sci. U. S. A.* **107**, 13666–13671
29. Yu, B., Gu, L., and Simon, M. I. (2000) Inhibition of subsets of G protein-coupled receptors by empty mutants of G protein alpha subunits in g(o), G(11), and G(16). *J. Biol. Chem.* **275**, 71–76
30. Sauliere, A., Bellot, M., Paris, H., Denis, C., Finana, F., Hansen, J. T., *et al.* (2012) Deciphering biased-agonism complexity reveals a new active AT1 receptor entity. *Nat. Chem. Biol.* **8**, 622–630
31. Okashah, N., Wright, S. C., Kawakami, K., Mathiasen, S., Zhou, J., Lu, S., *et al.* (2020) Agonist-induced formation of unproductive receptor-G12 complexes. *Proc. Natl. Acad. Sci. U. S. A.* **117**, 21723–21730
32. Tang, H., Shirai, H., and Inagami, T. (1995) Inhibition of protein kinase C prevents rapid desensitization of type 1B angiotensin II receptor. *Circ. Res.* **77**, 239–248
33. Ostrom, R. S., and Insel, P. A. (2004) The evolving role of lipid rafts and caveolae in G protein-coupled receptor signaling: implications for molecular pharmacology. *Br. J. Pharmacol.* **143**, 235–245
34. Wingler, L. M., Elgeti, M., Hilger, D., Latorraca, N. R., Lerch, M. T., Staus, D. P., *et al.* (2019) Angiotensin analogs with divergent bias stabilize distinct receptor conformations. *Cell* **176**, 468–478.e411
35. Harris, J. A., Faust, B., Gondin, A. B., Damgen, M. A., Suomivuori, C. M., Veldhuis, N. A., *et al.* (2022) Selective G protein signaling driven by substance P-neurokinin receptor dynamics. *Nat. Chem. Biol.* **18**, 109–115
36. Wirth, A., Benyo, Z., Lukasova, M., Leutgeb, B., Wettschureck, N., Gorbey, S., *et al.* (2008) G12-G13-LARG-mediated signaling in vascular smooth muscle is required for salt-induced hypertension. *Nat. Med.* **14**, 64–68
37. Althoff, T. F., Albarran Juarez, J., Troidl, K., Tang, C., Wang, S., Wirth, A., *et al.* (2012) Procontractile G protein-mediated signaling pathways antagonistically regulate smooth muscle differentiation in vascular remodeling. *J. Exp. Med.* **209**, 2277–2290

38. Mir, F. M., Atmuri, P. N. D., Bourguet, C. B., Fores, J. R., Hou, X., Chemtob, S., *et al.* (2019) Paired utility of aza-amino acyl proline and indolizidinone amino acid residues for peptide mimicry: conception of prostaglandin F2α receptor allosteric modulators that delay preterm birth. *J. Med. Chem.* **62**, 4500–4525
39. Gales, C., Rebois, R. V., Hogue, M., Trieu, P., Breit, A., Hebert, T. E., *et al.* (2005) Real-time monitoring of receptor and G-protein interactions in living cells. *Nat. Met.* **2**, 177–184
40. Avet, C., Sturino, C., Grastilleur, S., Gouill, C. L., Semache, M., Gross, F., *et al.* (2020) The PAR2 inhibitor I-287 selectively targets Galphaq and Galpha12/13 signaling and has anti-inflammatory effects. *Commun. Biol.* **3**, 719
41. Gagnon, L., Cao, Y., Cho, A., Sedki, D., Huber, T., Sakmar, T. P., *et al.* (2019) Genetic code expansion and photocross-linking identify different beta-arrestin binding modes to the angiotensin II type 1 receptor. *J. Biol. Chem.* **294**, 17409–17420
42. Heydenreich, F. M., Miljus, T., Jaussi, R., Benoit, R., Milic, D., and Veprintsev, D. B. (2017) High-throughput mutagenesis using a two-fragment PCR approach. *Sci. Rep.* **7**, 6787
43. Devost, D., Sleno, R., Petrin, D., Zhang, A., Shinjo, Y., Okde, R., *et al.* (2017) Conformational profiling of the AT1 angiotensin II receptor reflects biased agonism, G protein coupling, and cellular context. *J. Biol. Chem.* **292**, 5443–5456
44. Zimmerman, B., Beautrait, A., Aguila, B., Charles, R., Escher, E., Claing, A., *et al.* (2012) Differential beta-arrestin-dependent conformational signaling and cellular responses revealed by angiotensin analogs. *Sci. Signal.* **5**, ra33